Spatial Correlation in Ultrawideband Channels

Wasim Q. Malik, *Member, IEEE*

***Abstract*— Correlated fading adversely affects the spatial multiplexing and diversity performance of multiple-antenna systems. This paper presents an empirical investigation of spatial correlation in ultrawideband (UWB) indoor channels in the FCC-allocated 3.1–10.6 GHz band. The impact of a number of system parameters on spatial correlation at the receiver is evaluated. It is found that the coherence distance falls with channel bandwidth in endfire arrays but not in broadside arrays. The complex correlation decays less rapidly with distance in broadside arrays than in endfire arrays, especially under line-of-sight, but the envelope correlation is circularly symmetric in space. Strong dependence of spatial correlation and coherence distance on the channel center frequency is observed. Furthermore, horizontally polarized links are found to exhibit less correlation than vertically polarized links. A discussion of the implications of these results for multiple-antenna UWB systems is provided.**

***Index Terms*— Antenna arrays, multiple-input multiple-output (MIMO), spatial correlation, ultrawideband (UWB).**

I. Introduction

MULTIPLE-input multiple-output (MIMO) techniques are propelling the advances in wireless communications, with the promise of very high data-rates and robustness [1], [2]. The spatial correlation in the multipath channel is a critical factor in the performance of a MIMO system. The fading correlation between the array elements should be sufficiently low for a MIMO system to offer any performance enhancement [3]. High correlation between multiple signal streams can reduce the channel matrix rank; a perfectly correlated channel has unit rank with a single effective degree of freedom. Any potential diversity or spatial multiplexing advantage is then lost, and the performance reduces to that of a single-input single-output (SISO) system. Correlation not only affects the performance of spatial arrays but also that of angular and polarized arrays [4], [5]. In this paper, however, we will limit our discussion to correlation in the spatial domain, analyzing its characteristics given a uniform linear or rectangular array of identical antenna elements. The results presented are also applicable to other spatial array topologies and to virtual arrays formed by cooperative nodes. Another application of this analysis is in wireless positioning systems that rely on the database correlation method using the channel response as the unique location fingerprint [6].

Several factors determine the degree of spatial correlation, such as array element spacing [7], transmitter-receiver separation [8], [9], array orientation [10], and multipath angular spread [11]. Degenerate MIMO channels, for example, offer only a single spatial degree of freedom due to the keyhole effect [1], [12]. In a typical scattering environment, spatial correlation can be reduced to the desired level by designing the antenna array with sufficient inter-element spacing, d. Conversely, the optimal value of the array design parameter d is obtained by analyzing the channel correlation characteristics.

The correlation properties of narrowband MIMO channels are well understood. Thus, in a Rayleigh fading channel with rich, isotropic scattering, the envelope correlation, ρ, is related to the antenna spacing, d, and carrier frequency, f, through a zeroth order Bessel function of the first kind, i.e. [2]

$$\rho(d, f) = J_0(2\pi d/\lambda), \tag{1}$$

where $\lambda = c/f$ is the wavelength and c is the speed of light. A half-wavelength spacing is therefore considered an ideal choice for minimizing the correlation without greatly increasing the physical dimensions of the array. However, when the scattering is sparse and non-isotropic, ρ does not fall quite so rapidly with d. The coherence distance, D_c, then increases, and a much larger d may be required to achieve sufficient decorrelation [13].

The propagation characteristics of ultrawideband (UWB) channels, however, differ greatly from those of conventional narrowband channels [14]. The impact of various system and channel parameters on UWB spatial correlation is not completely known at present, and is the main focus of this paper. A departure from the narrowband characteristics is expected owing to the differences in the propagation mechanisms, and the peculiar characteristics of spatial correlation in indoor UWB channels thus merit special attention. This characterization is especially important due to the increasing popularity of UWB communications technology and its imminent deployment in wireless networks, consumer electronics applications, and sensors. Since the recent enactment of radio regulations in many countries permitting unlicensed UWB operation, it has become a leading contender for high-rate indoor wireless systems [15]. MIMO technology, exploiting physical or virtual antenna arrays, has the potential to substantially enhance the data-rates achievable by UWB [5], catering to high-end applications such as wireless multimedia transmission or sensor networks with high spatial density. An understanding of the UWB spatial channel, and its correlation characteristics in particular, is thus of paramount importance for future wireless communications.

In this paper, a comprehensive analysis of UWB spatial correlation is undertaken based on channel measurements in the 3.1–10.6 GHz band allocated by the Federal Communications Commission (FCC) in the United States. Previous studies have modelled the correlation as a function of frequency on

Manuscript received August 4, 2006; revised July 21, 2007; accepted November 8, 2007. The associate editor coordinating the review of this paper and approving it for publication was R. M. Buehrer. This work was supported in part by the ESU Lindemann Trust and the UK Engineering and Physical Sciences Research Council via Grant GR/T21769/01.

W. Q. Malik is with the Laboratory for Information and Decision Systems, Massachusetts Institute of Technology, 77 Massachusetts Avenue, Cambridge, MA 02139 USA (e-mail: wqm@mit.edu).

Digital Object Identifier 10.1109/TWC.2008.060547.

a single-frequency basis, which is essentially a narrowband treatment [16], [17]. In contrast, our analysis of frequency dependence is based on the frequency-domain correlation of true UWB channels meeting the FCC definition. We also establish the relationship between the receive correlation and the receiving array elemental spacing for both broadside and endfire arrays using local spatial variation analysis. Another contribution of this paper is an analysis of the dependence of correlation on channel bandwidth. Finally, the effect of link polarization on the correlation characteristics is analyzed.

We restrict our analysis in this paper to receive correlation. If link reciprocity is assumed, the transmitter and receiver can be expected to experience similar scattering environments, and therefore similar spatial correlation characteristics. Such a situation is likely to be encountered in typical UWB applications, e.g. peer-to-peer indoor networks or interconnects such as wireless USB. Under this condition of reciprocity, our analysis and results will also hold for transmit correlation.

II. System Model and Channel Measurement

Using a vector network analyzer (VNA), coherent frequency-domain measurements are performed over the FCC-allocated 7.5 GHz wide UWB band centered at 6.85 GHz (i.e., $f_l = 3.1$ GHz to $f_h = 10.6$ GHz). With $F = 1601$ discrete frequency points to sample the channel, the frequency resolution, $\Delta f = W/(F-1) \approx 4.7$ MHz, is much smaller than the channel coherence bandwidth. The measurement apparatus, consisting of the VNA, amplifiers, cables and connectors, is calibrated to remove frequency-selective attenuation and phase rotation. Discone antennas with efficient radiation characteristics over the UWB band are used [18]. The antennas, which are linearly polarized and have omnidirectional power radiation patterns, are placed at a height of 1.5 m. The antenna pair is rotated to obtain the vertically (V) and horizontally (H) polarized channels, following the procedure used in [5].

For typical broadcast antennas with omni-directional radiation in azimuth, antenna polarization rotation is inevitably accompanied with radiation pattern alteration. Our analysis of polarization effects on correlation thus implicitly includes pattern rotation and the consequent variations in the multipath profile of the channel excited by an antenna with non-isotropic directivity [19]. The spatial correlation experienced by a given UWB device may also be affected by its particular antenna characteristics, such as non-omnidirectional radiation or pattern distortion due to device integration [20], as multipath angular spread reduction leads to higher correlation [13].

Our spatial channel analysis is based on virtual antenna arrays at the receiver, with a fixed transmitter. A computer-controlled positioning grid is used to scan a 1 m $\times$ 1 m area. With this arrangement, receiving linear arrays are synthesized in both broadside and endfire configurations with minimum inter-element spacing $d = 1$ cm, maximum aperture width $D = 1$ m, and up to $N_d = 100$ elements, as illustrated in Fig. 1. Due to aperture synthesis, this analysis does not include the effects of antenna coupling [21], and the scope of the current discussion is limited to correlation analysis. Measurements of both unobstructed line-of-sight (LOS) and non-LOS (NLOS) indoor propagation scenarios are conducted.

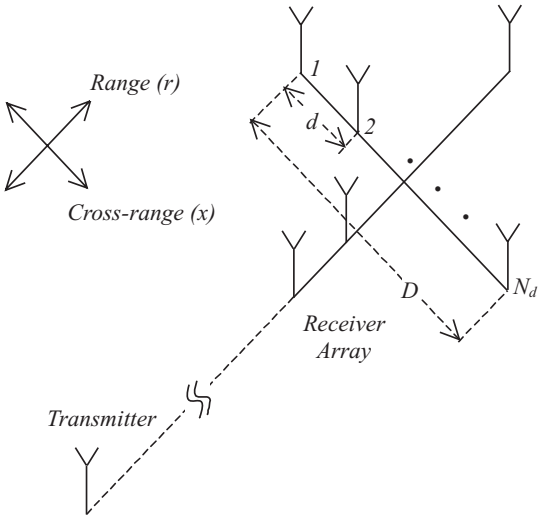

Fig. 1. The N_d-element receive antenna array with inter-element spacing d and aperture width D.

The time stationarity of the channel is a requirement for the validity of the array synthesis approach, and is ensured by completely immobilizing the measurement environment, as established in [5]. This is in line with previous studies demonstrating the time stationarity of indoor office and residential environments [22]. A different operating scenario, such as an outdoor UWB channel, may not exhibit time stationarity, and the spatial correlation characteristics may then vary in time.

Several indoor small-office environments with dimensions of the order of 6 m $\times$ 6 m and dense multipath are measured. The locations within the rooms are varied, and the transmitter-receiver separation ranges from 3 to 6 m. Representing the receiving antenna position on the Cartesian measurement grid by the cross-range, x, and range, r, components, and the corresponding sets of locations by X and R, respectively, we can express the complex channel transfer function (CTF) as

$$H(r,x,f) = \sum_{k=0}^{F-1} A(r,x,k) e^{j\phi(r,x,k)} \delta(f - k\Delta f), \quad (2)$$

where $r \in R$ is the range location, $x \in X$ is the cross-range location, A is the amplitude and ϕ is the phase. Under this representation, various values of $x \in X$, with r being constant, define a broadside array, etc.

III. Spatial Correlation Evaluation

In this paper, the spatial correlation coefficient, ρ, is calculated from the set of measured channel responses in the frequency domain. The receive correlation coefficient signifies the statistical correlation between the signals received at two different locations after being emitted by the same transmitter, while the transmit correlation is the converse quantity, i.e. the correlation with two transmitters and one receiver. Consider two complex CTFs, $H_1 = H(r_1, x_1, f)$ and $H_2 = H(r_2, x_2, f)$, measured at locations (r_1, x_1) and (r_2, x_2), respectively, separated by distance, d, given by

$$d = \sqrt{(r_2 - r_1)^2 - (x_2 - x_1)^2}. \quad (3)$$

The degree of similarity between these two CTFs can be estimated in terms of their cross-correlation. We note that the CTF is a random process as the frequency-domain fading coefficients are stochastic. Now, the correlation coefficient, ρ, between two complex random variables $u(\xi)$ and $v(\xi)$ can be evaluated using the general expression [5], [8]

$$\rho(u,v) = \frac{\mathcal{E}\left\{uv^{\dagger}\right\} - \mathcal{E}\left\{u\right\}\mathcal{E}\left\{v^{\dagger}\right\}}{\sigma_u \sigma_v} \tag{4}$$

where $\mathcal{E}(.)$ denotes expectation, $(.)^{\dagger}$ denotes conjugation,

$$\sigma_u = \sqrt{\left(\mathcal{E}\left\{|u|^2\right\} - |\mathcal{E}\left\{u\right\}|^2\right)} \tag{5}$$

and σ_v is defined in a similar manner. In order to calculate the complex correlation coefficient, ρ_c, for the UWB channel using the CTFs, we use (4) and (5) with $u = H_1$, $v = H_2$ and $\xi = f$. The envelope correlation, ρ_e, and power correlation, ρ_p, defined in [8], provide alternative definitions of the correlation coefficient. However, ρ_e and ρ_p do not make use of the phase information in the complex CTFs. To calculate ρ_e, we put $u = |H_1|$ and $v = |H_2|$ in (4) and (5), while for ρ_p, we use $u = |H_1|^2$ and $v = |H_2|^2$. The approximation

$$\rho_p \approx \rho_e \approx |\rho_c|^2 \tag{6}$$

holds for Rayleigh-faded narrowband wireless channels [3], but not necessarily for other fade distributions.

We evaluate these three types of correlation for UWB channels, analyzing the effect of array orientation, signal polarization and propagation scenario. Our treatment therefore identifies two distinct cases of array orientation, *viz* broadside (cross-range correlation) and endfire (range correlation), each expressed as a function of the spatial offset, d. In radio channels with small angular spread, the arrays are designed to operate in the broadside direction, which leads to better performance than that obtained with endfire arrays [7]. If the angular spread is large, the performance difference between broadside and endfire arrays is reduced. If the channel is asymptotically isotropic in the horizontal plane, the correlation becomes a two dimensional Bessel function of d with contours circularly symmetric about the point of reference [23]. Fortunately, indoor UWB channels typically exhibit large angular spreads [14], which is also reflected in our measurements.

A. Cross-range Correlation

According to the above channel formulation and on invoking the plane wave assumption, the cross-range dimension, x, signifies a broadside receive antenna array for a given range, r. In order to evaluate the cross-range correlation coefficient, ρ, at a given range r, we extract a single row of CTFs, $H_i = H(r,i,f)$, where $i \in X$, $i = \{1,\ldots,N_d\}$. Since we are interested in investigating the variation of ρ with the cross-range inter-element spacing d, we designate the central antenna element of the r^{th} row, i.e. $i_0 = N_d/2$, as the reference location[1]. We cross-correlate the corresponding reference CTF, $H_0 = H(r,i_0,f)$, with H_i to obtain $\rho = \langle H_i, H_0 \rangle$ for the r^{th} range location. The process is repeated for all $r \in R$. The

[1]If N_d is even, either of the two central points can be used as the reference for this analysis.

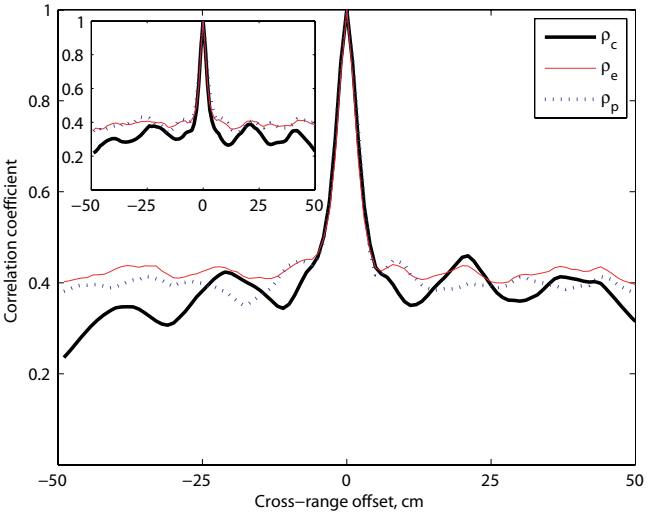

(a) along cross-range direction with vertical polarization

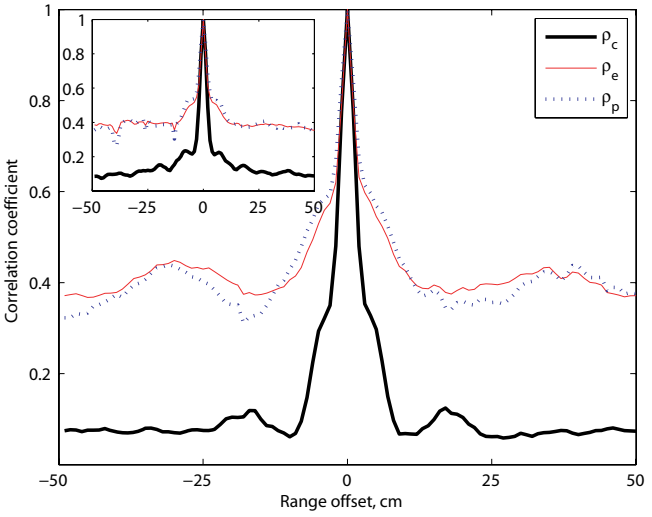

(b) along range direction with vertical polarization

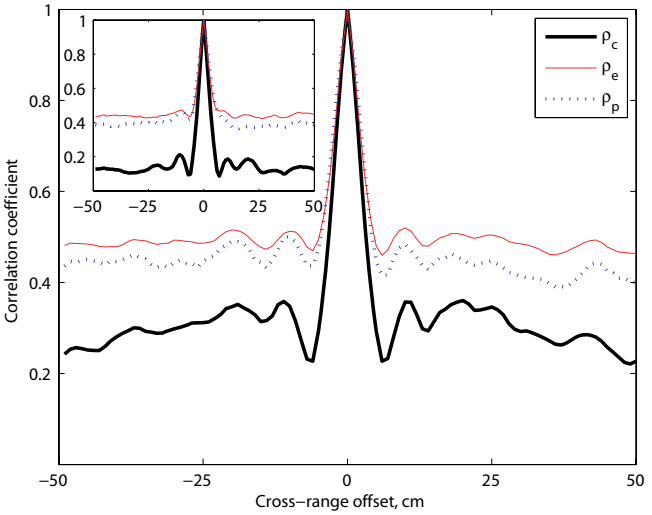

(c) along cross-range direction with horizontal polarization

Fig. 2. The average spatial correlation magnitude verses the spatial offset in LOS with the specified offset direction and antenna polarization. The insets show the correlation for the corresponding NLOS channels. The complex (ρ_c), envelope (ρ_e) and power (ρ_p) correlation values are shown.

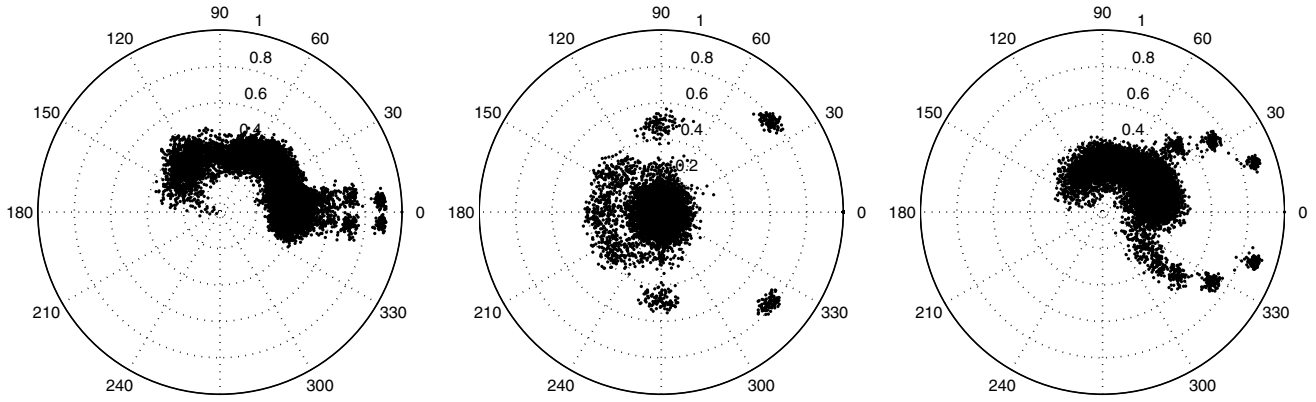

(a) cross-range, vertical polarization (b) range, vertical polarization (c) cross-range, horizontal polarization

Fig. 3. The spatial correlation magnitude and phase distribution in the LOS channel with the specified offset direction and antenna polarization.

mean spatial correlation is evaluated as a function of cross-range distance (i.e. for a given i) by averaging across R.

We calculate the complex, envelope and power correlations as functions of the cross-range offset. Fig. 2 shows the mean correlation magnitudes for the UWB channel with $W = 7.5$ GHz and $f_c = 6.85$ GHz. From inspection, the complex correlation in Fig 2(a) appears to follow a pattern resembling a Bessel function of d. The trends of the envelope and power correlation are approximately similar to each other as predicted by (6). It is noteworthy that the square-law relation between the envelope and complex correlation in (6), valid for narrowband channels, does not appear to hold for the UWB channel. A possible reason is that the UWB channel does not exhibit Rayleigh fading characteristics [14], and this in turn impacts the relationship between the various types of the correlation coefficient. Detailed analysis of UWB channel fading distribution is, however, beyond the scope of this paper and we will not investigate this observation further.

Also from Fig. 2, the NLOS correlation is smaller as the scattering becomes more isotropic, however this difference is not substantial. The H channel has a significantly lower ρ_c than the V channel, as seen from Fig. 2(c), but the difference is less apparent for ρ_e and ρ_p. From Fig. 2(a), the distance between the peak and the first local minimum of $|\rho_c|$ is 11 cm. The coherence distance, D_c, defined as the distance within which $|\rho_c| \geq 0.5$, is approximately 4 cm. Similar D_c is observed for LOS and NLOS scenarios and for V and H polarizations.

Fig. 3 analyzes the phase component of ρ_c for the UWB channel using a polar representation similar to that used in [8] for narrowband channels. The correlation coefficient phase, $\angle\rho_c$, provides information about the dominant multipath directions-of-arrival (DOAs) [2, Sec. 2.1.6], since a translation in the direction of wave propagation will introduce a phase lag to ρ_c. In Fig. 3(a), the conjugate pairs with $|\rho_c| \geq 0.8$ are obtained at the values of d for which the correlation peaks appear in Fig. 2(a). Also, $\angle\rho_c$ lies predominantly in the upper half plane, i.e., $[0, 180°]$. The reason is that the reference location is closer to the transmitter compared to other cross-range locations. With the aperture size and transmitter-receiver separation considered, the far-field array condition is not satisfied in a strict sense, and the direct arrival is actually a spherical wave over the full cross-range span of the measurement grid. The direct wave therefore traverses the shortest distance to reach the reference location than to reach any other location in the same cross-range row. A corresponding phase lag is thus observed at the off-reference locations, which appears as a positive phase in the correlation coefficient. At a large transmitter-receiver separation, $\angle\rho_c$ will be uniformly distributed. Also, in the NLOS channel (result not shown), $\angle\rho_c$ is more uniformly distributed as the direct component in no longer so dominant. The trends observed in the H channel, as seen from Fig. 3(c), bear broad similarity.

B. Range Correlation

We now extend our analysis to the spatial correlation characteristics in the range direction, which signifies the performance of endfire arrays. In order to achieve this, we calculate the expectation, over the measurement ensemble, of the spatial correlation coefficient for a given range offset. The latter, in turn, is evaluated in terms of the correlation coefficient between the central element of the x^{th} column of the spatial measurement grid and the other elements in that column.

The mean correlation coefficient magnitudes thus obtained are shown in Fig. 2(b). It is observed that $\rho_e \approx \rho_p$ for all d. The range correlation has a broader mainlobe support compared with the cross-range correlation. The first null of ρ_e and ρ_p is obtained at $d = 13$ cm approx., while the $|\rho| = 0.5$ threshold is crossed at $d = 7$ cm. However, ρ_e and ρ_p do not fall much lower than $|\rho| = 0.4$, even for large d. In contrast, ρ_c decays rapidly, reaching a steady value of $|\rho| \approx 0.1$ at $d = 8$ cm after which the oscillations are relatively insignificant. Also, $d = 2$ cm is found to be sufficient for $|\rho_c| \leq 0.5$. No significant differences are observed between LOS and NLOS channels.

Fig. 3(b) shows a polar coordinate representation of ρ_c. The values $|\rho| \approx 0.8$ and $\angle\rho \approx \pm 40°$ are obtained at the spatial locations close to the reference locations. This conjugate symmetry at the range locations on either side of the reference location arises due to the corresponding phase lag and lead in the direct wave. The next set of points on either side of the reference give rise to the conjugate pair with $|\rho| \approx 0.5$ and $\angle\rho \approx \pm 90°$. The rest of the locations produce

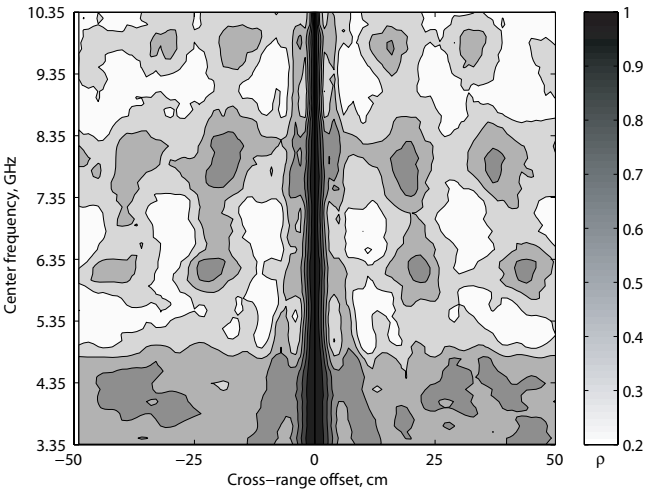

(a) along cross-range direction

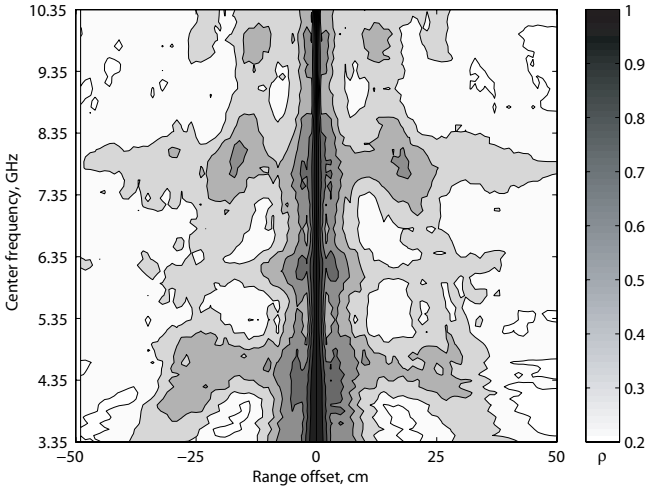

(b) along range direction

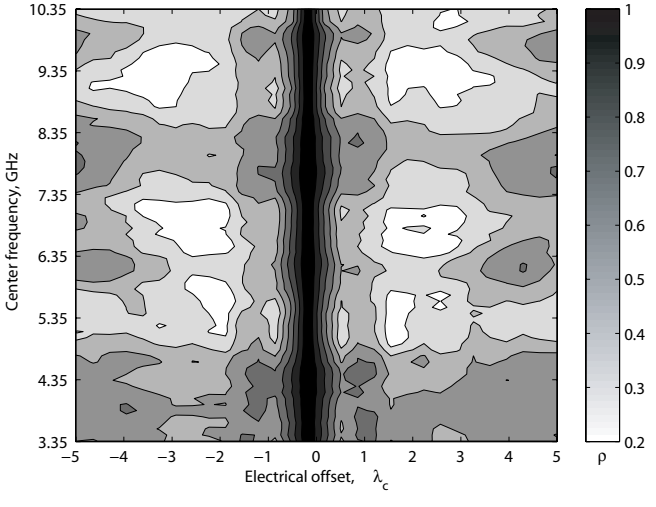

(c) along cross-range direction

Fig. 4. Variation of mean spatial correlation magnitude with center frequency in the vertically polarized LOS UWB channel, with the spatial offset, d, in the specified direction. An alternative representation of (a) is given in (c), showing the dependence on electrical offset in number of wavelengths.

ρ_c with smaller magnitude and almost uniformly distributed phase.

To summarize this section, D_c is approximately 4 cm for most full-band UWB channels. This value of D_c is close to the half-wavelength span of the lowest frequency component, $f_l = 3.1$ GHz, in agreement with intuition. Also, while LOS blockage lowers the correlation, the effect is not as dramatic as in channels with comparatively narrow bandwidth; see, for example, [11]. In terms of the envelope or power correlation, greater antenna separation is required in the endfire arrays than in broadside arrays for sufficient signal decorrelation.

In the rest of this paper, we will consider only the complex correlation coefficient and drop the subscript for notational simplicity, representing the complex correlation simply by ρ.

IV. Impact of System Parameters

We next investigate the impact of some system parameters on spatial correlation, *viz* the center frequency, f_c, and bandwidth, W. The effect on both broadside and endfire arrays is characterized. Considering ρ as a function of d in the cross-range direction, N_d is the number of elements in the range direction, H_0 is taken at location (x_0, y_n), and H_i is taken at the i^{th} location along the n^{th} row over the measurement grid, where x_0 is the middle element of that row. An equivalent definition is used to evaluate the correlation along the range.

A. Center Frequency

We commence by characterizing the effect of center frequency, f_c, on spatial correlation. We also investigate the dependence of coherence distance, D_c, on f_c by defining

$$N_\lambda = \lambda_c / D_c, \tag{7}$$

where $\lambda_c = c/f_c$. Furthermore, we express the electrical distance at f_c between two points separated by physical distance d as $d_\lambda = d/\lambda_c$, where d_λ is a unitless quantity.

According to the Jakes model, narrowband spatial correlation varies with f_c as a Bessel function, given constant d, as expressed in (1). To our knowledge, no results on the dependence of correlation on f_c are available in literature that are based on UWB channels. The empirical attempts in [16], [17] are derived from essentially narrowband techniques, as they consider the correlation behavior for the individual frequency components. In [16], D_c is shown to decrease with increasing f_c in 2–8 GHz NLOS channels, as expected, but the reverse trend is reported for LOS channels. No physical explanation for this counter-intuitive observation is offered, and the reliability of the results is also put into question by the authors. According to the trends in [17], D_c varies inversely with f_c in the 1.4–3.4 GHz band, and N_λ is reported to be 3.5 and 4 for LOS and NLOS channels, respectively. This result is comparable to the relation for narrowband Rayleigh-faded channels, for which $D_c \approx 9\lambda/16\pi \Rightarrow N_\lambda \approx 5.5$ [13].

We investigate the relationship of ρ and f_c using true UWB channels with bandwidth fixed at the FCC's lower limit of $W = 500$ MHz. The center frequency is varied from 3.35 GHz to 10.35 GHz so that the UWB channel follows the FCC UWB spectrum boundaries. The 500 MHz channels are extracted from the 7.5 GHz measured channels using an ideal bandpass filter with 500 MHz bandwidth translated to the desired f_c.

The correlation dependence of broadside arrays on f_c is illustrated by Fig. 4(a). For a given f_c, ρ is a decaying oscillatory function of d resembling the Bessel function. Strong correlation sidelobes, some of which may lie above the $|\rho| = 0.5$ threshold, appear and disappear with f_c at constant d. For the endfire array, the sidelobes are less pronounced, the functional compression with increasing f_c is more noticeable, and in general the correlation values are lower, as seen in Fig. 4(b). The sidelobe levels and widths in NLOS are somewhat lower along both range and cross-range, due to greater scattering, but the difference is insignificant. Polarization analysis shows that the H channel is comparatively less correlated than the V channel. This is also due to the greater pathloss and delay spread experienced by H channels in our measurements.

Also, from Fig. 4, D_c appears to be inversely related to f_c. We study the variation of ρ with d_λ, and their direct relationship is indeed observed in Fig. 4(c). Further analysis shows that ρ attains its lowest value at $d_\lambda \approx 2$. We undertake this investigation for various array orientations, propagation scenarios and polarizations, and quantify the results in terms of N_λ. Detailed analysis reveals that $N_\lambda \approx 1$, or $D_c \approx \lambda_c$, for all of the channel combinations considered, using the $|\rho| = 0.5$ threshold. Thus, for the UWB channel, the coherence distance is of the order of the central wavelength. This result is especially important for multiband UWB systems, as it implies that the coherence distance, and indeed the spatial correlation, will vary depending on the subband under use. Operating exclusively in the higher subbands will facilitate the deployment of compact ULAs in MIMO UWB systems.

B. Bandwidth

The impact of channel bandwidth, W, on spatial correlation has not been investigated in the literature, to the author's knowledge. We now undertake this analysis, for which the channel center frequency is fixed at $f_c = (f_l + f_h)/2 = 6.85$ GHz, while W is varied. For the i^{th} measurement location on the grid, we extract the CTF, H_i, corresponding to the desired frequency band, which is then cross-correlated with the reference CTF, H_0, of the same bandwidth. The spatial averaging and analysis procedure is the same as described earlier, and the mean correlation coefficient is obtained as a function of d along cross-range and range. In order to compare UWB spatial correlation to that of narrowband and wideband channels, we vary W from 25 MHz to 7.5 GHz.

Fig. 5(a) shows the mean ρ at a given cross-range offset d as a function of W. In the UWB channel ($W \geq 500$ MHz), ρ exhibits an oscillatory behavior as a function of d. We find that ρ is minimized at $d \approx 10$ cm. It is also observed that $D_c \approx 4$ cm, which is in close agreement with the findings of Sec. IV-A, as $f_c = 6.85$ GHz here, so that $\lambda_c = 4.4$ cm and $D_c \approx \lambda_c$. No significant changes are observed in the cross-range correlation at $W \geq 1$ GHz, therefore there appears to be little gain from occupying the full available bandwidth as far as spatial correlation is concerned. When d is constant, ρ falls almost monotonically but not linearly with an increase in W, for both range and cross-range. For the wideband channel (25 MHz $\leq W \leq$ 100 MHz), $\rho \geq 0.5$ even at large d. In fact, ρ does not vary significantly with W beyond $W = 0.5$ GHz.

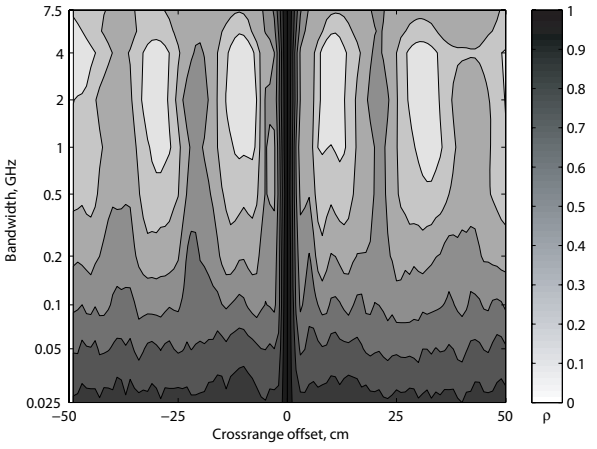

(a) along cross-range direction

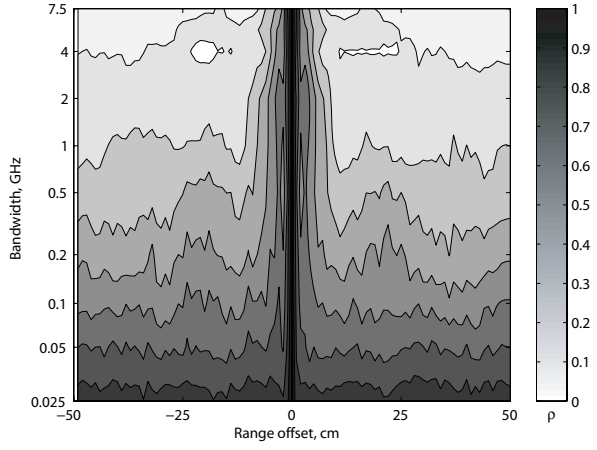

(b) along range direction

Fig. 5. The variation of mean spatial correlation magnitude with bandwidth in the vertically polarized LOS UWB channel.

The minimum ρ is achieved at $d \approx 10$ cm $\forall$ W. Further analysis and modelling reveals that a decaying exponential function provides a close approximation of the dependence of ρ on $\log_{10} W$ for various array orientations and elemental separations.

There is no evidence of an appreciable effect of W on the correlation mainlobe width. In the H channel, the correlation sidelobes are significantly smaller for all W in the cross-range direction, while the behavior along the range is similar to that observed in the vertical channels at various values of W.

V. Discussion and Conclusion

Correlation characteristics depend jointly on the array orientation and the multipath angular spread. In some outdoor mobile channels, the elemental spacing requirement for an endfire array may be as high as four-fold that of a broadside array [7], in turn affecting the MIMO capacity [10]. From our results, endfire arrays are more favorable than broadside arrays in an LOS scenario when complex correlation is considered, since the co-phased LOS wavefronts impinging on the broadside array raise the correlation. The orientation is less significant in NLOS due to greater scattering and larger angular

spreads. Realistic indoor UWB channels typically exhibit large angular spreads. Therefore a symmetric or quasi-symmetric array topology is unlikely to boost MIMO performance very significantly, in contrast with low angular spread channels.

This paper has investigated the spatial correlation in the indoor UWB channel using measurements with omnidirectional antennas. It is shown that the complex correlation properties depend on the array orientation, while the envelope and power correlation are circularly symmetric in the azimuth plane. With a broadside UWB array, the complex correlation is a decaying, oscillatory function of the distance between the elements, similar to narrowband channels. With an endfire array, however, it decays approximately exponentially with distance. For a UWB signal, the spatial correlation is a decaying exponential function of the channel bandwidth. Furthermore, the channel coherence distance is shown to be equivalent to the wavelength corresponding to the center frequency, and is therefore nonuniform across the subbands in a multiband UWB system. The use of directional antennas, antenna pattern distortion due to device integration, or low angular spread in the propagation environment can increase the spatial correlation significantly. However, with an inter-element spacing requirement of a few centimeters, the deployment of MIMO arrays in compact UWB devices appears to be commercially feasible.

ACKNOWLEDGMENT

The author is grateful to Prof. Andreas Molisch, Prof. David Edwards and Dr. Ben Allen for their insightful comments.

REFERENCES

[1] A. J. Paulraj, R. Nabar, and D. Gore, *Introduction to Space-Time Wireless Communications*. Cambridge, UK: Cambridge University Press, 2003.

[2] C. Oestges and B. Clerckx, *MIMO Wireless Communications*. Orlando, FL: Academic Press, 2007.

[3] R. O. LaMaire and M. Zorzi, "Effect of correlation in diversity systems with Rayleigh fading, shadowing, and power capture," *IEEE J. Select. Areas Commun.*, vol. 14, no. 3, Apr. 1996.

[4] J. Jootar, J.-F. Diouris, and J. R. Zeidler, "Performance of polarization diversity in correlated Nakagami-m fading channels," *IEEE Trans. Veh. Technol.*, vol. 55, no. 1, Jan. 2006.

[5] W. Q. Malik and D. J. Edwards, "Measured MIMO capacity and diversity gain with spatial and polar arrays in ultrawideband channels," *IEEE Trans. Commun.*, vol. 55, no. 12, Dec. 2007.

[6] W. Q. Malik and B. Allen, "Wireless sensor positioning with ultrawideband fingerprinting," in *Proc. Eur. Conf. Antennas Propagat. (EuCAP)*, Edinburgh, UK, Nov. 2007.

[7] W. C. Y. Lee, *Mobile Communications Engineering*. New York: McGraw-Hill, 1982.

[8] P. Kyritsi, D. C. Cox, R. A. Valenzuela, and P. W. Wolniansky, "Correlation analysis based on MIMO channel measurements in an indoor environment," *IEEE J. Select. Areas Commun.*, vol. 21, no. 5, June 2003.

[9] M. Chamchoy, S. Promwong, P. Tangtisanon, and J.-I. Takada, "Spatial correlation properties of multiantenna UWB systems for in-home scenarios," in *Proc. Int. Symp. Commun. Inform. Technol.*, Sapporo, Japan, Oct. 2004.

[10] D.-S. Shiu, G. J. Foschini, M. J. Gans, and J. M. Kahn, "Fading correlation and its effect on the capacity of multielement antenna systems," *IEEE Trans. Commun.*, vol. 48, no. 3, Mar. 2000.

[11] A. Intarapanich, P. L. Kafle, R. J. Davies, A. B. Sesay, and J. McRory, "Spatial correlation measurements for broadband MIMO wireless channels," in *Proc. IEEE Veh. Technol. Conf. (VTC)*, Los Angeles, CA, USA, Sept. 2004.

[12] P. Almers, F. Tufvesson, and A. F. Molisch, "Measurement of keyhole effect in a wireless multiple-input multiple-output (MIMO) channel," *IEEE Commun. Lett.*, vol. 7, no. 8, Aug. 2003.

[13] G. D. Durgin and T. S. Rappaport, "Theory of multipath shape factors for small-scale fading wireless channels," *IEEE Trans. Antennas Propagat.*, vol. 48, no. 5, May 2000.

[14] B. Allen, M. Dohler, E. E. Okon, W. Q. Malik, A. K. Brown, and D. J. Edwards, Eds., *Ultra-Wideband Antennas and Propagation for Communications, Radar and Imaging*. London: Wiley, 2006.

[15] S. Roy, J. R. Foerster, V. S. Somayazulu, and D. G. Leper, "Ultrawideband radio design: the promise of high-speed, short-range wireless connectivity," *Proc. IEEE*, vol. 92, no. 2, Feb. 2004.

[16] C. Prettie, D. Cheung, L. Rusch, and M. Ho, "Spatial correlation of UWB signals in a home environment," in *Proc. IEEE Conf. Ultra-Wideband Sys. Tech. (UWBST)*, Baltimore, MD, USA, May 2002.

[17] H. Agus, J. Nielsen, and R. J. Davies, "Correlation analysis for indoor UWB channel," in *Proc. Wireless 2005*, Calgary, AB, Canada, July 2005.

[18] W. Q. Malik, D. J. Edwards, and C. J. Stevens, "Angular-spectral antenna effects in ultra-wideband communications links," *IEE Proc.-Commun.*, vol. 153, no. 1, Feb. 2006.

[19] J. A. Dabin, N. Ni, A. M. Haimovich, E. Niver, and H. Grebel, "The effects of antenna directivity on path loss and multipath propagation in UWB indoor wireless channels," in *Proc. IEEE Conf. Ultra Wideband Sys. Tech. (UWBST)*, UWBST), Reston, VA, USA, Nov. 2003.

[20] D. Manteuffel, "Radio link characterization using real antenna integration scenarios for UWB consumer electronic applications," in *Proc. IET Symp. Ultra Wideband Sys. Tech. App.*, London, UK, Apr. 2006.

[21] J. W. Wallace and M. A. Jensen, "Mutual coupling in MIMO wireless systems: a rigorous network theory analysis," *IEEE Trans. Wireless Commun.*, vol. 3, no. 4, July 2004.

[22] H. Hashemi, "The indoor radio propagation channel," *Proc. IEEE*, vol. 81, no. 7, July 1993.

[23] G. L. Stüber, *Principles of Mobile Communications*, 2nd ed. Norwell, MA: Kluwer, 2001.

Wasim Q. Malik (M 2000) received the BE degree from the National University of Sciences and Technology, Pakistan, in 2000, and the DPhil degree from the University of Oxford, UK, in 2005, both in electrical engineering.

From 2005 to 2007, he was a Research Fellow at the University of Oxford, UK, and a Junior Research Fellow in Science at Wolfson College, Oxford. Since 2007, he has been a Postdoctoral Fellow at the Massachusetts Institute of Technology, USA.

Dr. Malik received the ESU Lindemann Science Fellowship 2007, the Best Paper Award at the ARMMS RF & Microwave Conference 2006, and the Association for Computing Machinery Recognition of Service Award in 1997. He is an editor of the book *Ultra-Wideband Antennas and Propagation for Communications, Radar and Imaging* (UK: Wiley, 2006), and a Guest Editor of the *IET Microwaves Antennas and Propagation* special issue on "antenna systems and propagation for future wireless communications" (Dec. 2007). He routinely serves on the organizing and technical program committees of various international conferences. He has published in excess of 60 papers in refereed journals and conferences.